

THE INFLUENCE OF A SHOCK ABSORBER ON DYNAMICS OF AN OFFSHORE PEDESTAL CRANE

JERZY KRUKOWSKI

National Oilwell Poland, Gdańsk, Poland

e-mail: jerzy.krukowski@nov.com

ANDRZEJ MACZYŃSKI, MAREK SZCZOTKA

University of Bielsko-Biala, Faculty of Management and Computer Science, Bielsko-Biala, Poland

e-mail: amaczyński@ath.bielsko.pl; mszczotka@ath.bielsko.pl

Offshore pedestal cranes are devices installed on offshore platforms or vessels. A characteristic feature of any floating object is the significant movement caused by sea waving. These movements cause that the offshore cranes are exposed to dynamic loads reasonably higher than structures of similar operational parameters but operated on land. Therefore, they are equipped with special systems for overload reduction. One of them is the shock absorber. The paper presents a mathematical model of an offshore pedestal crane with a shock absorber. Results of numerical simulations are presented to assess the effectiveness of the shock absorber in conditions when large dynamic overloads occur.

Key words: modelling, offshore crane, shock absorber

1. Introduction

Despite general economic slowdown in the world, we can still notice fast development of offshore technology connected with the exploration of underwater natural resources and its transport. Offshore devices are the ones assembled away from the shore line, usually on oil rigs and vessels. One of the major group is formed by offshore cranes.

One of the main features differentiating offshore devices from land-based devices is the significant movement of the base caused by sea waves. This phenomenon causes that they are exposed to much bigger dynamic overloads than their onshore counterparts. These overloads have significant influence on the permissible load capacity of the offshore crane. The aim of engineers is to design an offshore crane capable to work at possibly high rate of waving. As a result, a lot of emphasis is put on correct definition of dynamic overload appearing in this system. Hence, engineers, designers and analysts are interested in gaining access to the mathematical model of a crane which would allow one to perform fast calculations of crane dynamics in various conditions. Such simulations would be particularly useful at the early stage of the device development process.

We can find many publications connected with the modelling of the offshore crane dynamics in the literature. The authors develop models of different extent of details, 2D or 3D with rigid elements or those taking into account flexibility of chosen submodels. Operation of a winch in order to limit overload of a system or vertical movements of a load caused by the sea waving were considered by Osiński and Wojciech (1994, 1998). Similar issues were examined in the paper Pedrazzi and Barbieri (1998) concerning the cranes serving the purpose of launching Remotely Operated Vehicles. The stability of the load depth by means of an A-frame winch was the subject of papers: Fałat (2004), Adamiec-Wójcik *et al.* (2009). A 2D model of the system: supply vessel-load-crane-vessel, developed for the base and load dynamic analysis was presented by Osiński

et al. (2004). The nonlinear dynamical response to a regular waving of a crane mounted on the vessel was examined by Ellermann *et al.* (2002, 2003) and Ellermann and Kreuzer (2003). Both numerical simulations and experimental research were carried out. The possibility of parametric vibration of the crane under the influence of weak waving was analyzed by Witz (1995). The subject of consideration presented by Urbaś *et al.* (2010) was a gantry crane, installed on the oil platform. A mechanical anti-pendulum system was presented by Balachandran *et al.* (1999), Li and Balachandran (2001). Reduction of load swinging via proper steering of the crane slew and boom hoist was considered by Masoud (2000) and Nayfeh and Masoud (2004). A different concept of stabilizing the load position of an offshore crane was the subject of Maczyński (2005). Maczyński and Wojciech (2009) proved that stabilization of the load also minimizes the taut-slack phenomenon in a rope. Two different algorithms of control that minimize load waving were discussed by Schaub (2008). One of them was based on measurement data, the other one on generated calculations obtained from the numerical model of the system. The analyses presented by Cozijn *et al.* (2008) concentrated on the permissible work conditions for offshore installations including the offshore crane of S7000 type.

Currently designed offshore cranes are equipped with various systems that allow dynamic overloads to be reduced. One of the essential system is the shock absorber. However, the authors have not encountered any model in the literature which would include the existence of such a system.

2. Characteristics of a shock absorber

In the offshore crane design, two kinds of shock absorber systems are most commonly used. The first one is mounted on the boom structure of the crane. The minimalization of dynamic overload is obtained by leading the hoist rope through an additional sliding sheave connected with a hydraulic system. The other one, constituting the system of hydraulic accumulators, is mounted in the hook block. The subject of analysis presented in this work is the first type of the shock absorber because of its effectiveness, simple and compact construction.

Figure 1 shows in principle the hydraulic part of the shock absorber. It is the system consisting of an accumulator filled with gas and a hydraulic cylinder. When a force S applied to the piston is big enough, the piston is pulled out and oil is streaming from the cylinder to the accumulator. The end piston stroke length Δ_2 must normally be shorter than the maximum possible piston stroke length Δ_{max} minus a safety piston stroke length Δ_{safe} , to make sure there is no risk for the piston to reach the bottom at normal operation. The safety piston stroke length Δ_{safe} shall not be less than about 50 mm.

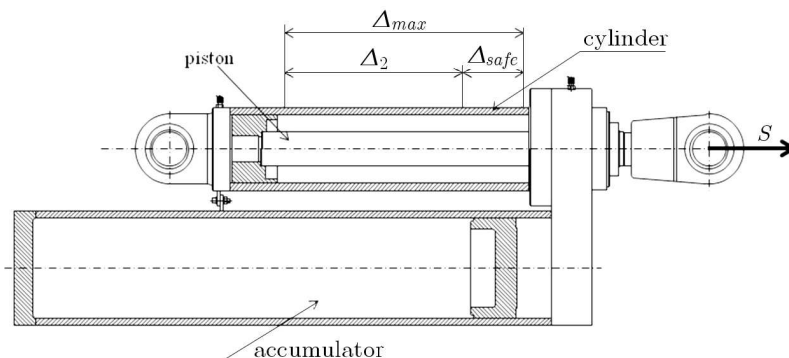


Fig. 1. Shock absorber

3. Model of the offshore crane

The subject of the paper is the offshore pedestal crane equipped with the system reducing dynamic overload, situated on the boom, see Fig. 2. The main assumptions adopted at the design stage and the most important connections used during derivation of the equation of motion will be given below. The modelling of the shock absorber was particularly emphasised. For the description of the system, joint coordinates and homogenous transformations were used based on the Denavit-Hartenberg notation.

In the model, the following assumptions were taken into consideration:

- The base of the crane (the platform of a vessel) and the supply vessel are rigid bodies with 6 degrees of freedom. The movement is caused by waving defined by pseudoharmonic functions.
- The pedestal, the A-frame and the boom are modelled by means of the Rigid Finite Element Method using a modified approach (MRFEM), (Wittbrodt *et al.*, 2006).
- The king frame, including the slewing part, is treated as a rigid structure with one degree of freedom with respect to the pedestal – the slew angle.
- The basic element of the shock absorber is the hydraulic cylinder, which was modelled as a point mass (additionally including the mass of the moving sheave) connected to the boom by means of a spring damping system.
- The hoist and the luffing ropes are modelled as massless elements with equivalent longitudinal flexibility. The damping was taken into account.
- The load is treated as a material point.
- The drive function of the hoist winch can be assumed in two ways: as a kinematic excitation or force excitation by a given moment.
- The luffing winch drive and the slew of the crane was adopted as a kinematic excitation.

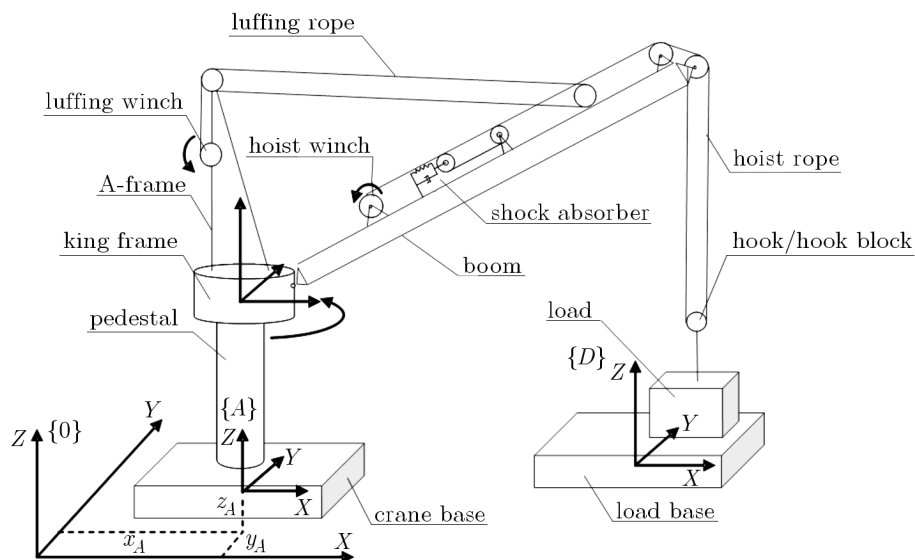


Fig. 2. Scheme of an offshore pedestal crane

The equations of motions were derived from the Lagrange equations of the second kind

$$\frac{d}{dt} \frac{\partial E}{\partial \dot{q}_k} - \frac{\partial E}{\partial q_k} + \frac{\partial V}{\partial q_k} + \frac{\partial D}{\partial \dot{q}_k} = Q_k \quad \text{for} \quad k = 1, \dots, n \quad (3.1)$$

where \mathbf{q} , $\dot{\mathbf{q}}$ are the vectors of generalized coordinates and their velocities, E , V – kinetic and potential energy, D – function of energy dissipation, Q_k – nonpotential generalized force corresponding to the k -th generalized coordinate, n – number of generalized coordinates.

3.1. Modelling of the crane and cargo base motion

It is assumed that the crane base motion and thus movement of the system $\{A\}$ with respect to the system $\{0\}$ is known and described by functions

$$y_i^{(A)} = \sum_{j=1}^{n_i^{(A)}} A_{i,j}^{(A)} \sin(\omega_{i,j}^{(A)} t + \varphi_{i,j}^{(A)}) \quad i = 1, \dots, 6 \quad (3.2)$$

where $A_{i,j}^{(A)}$, $\omega_{i,j}^{(A)}$, $\varphi_{i,j}^{(A)}$ are respectively the amplitude, phase, frequency and forcing phase angle, $n_i^{(A)}$ – number of harmonic series.

Motion of the supply vessel, i.e. system $\{D\}$, will be described in the same way.

In further considerations, the coordinate system $\{0\}$ will be identified with the inertial coordinate system $\{\cdot\}$, and the following notation will be used for the homogeneous transformation matrix from the coordinate system $\{p\}$ to the coordinate system $\{0\}$

$${}^0_p\mathbf{T} = \mathbf{T}^{(p)} \quad (3.3)$$

where p is the number of members in the kinematic chain.

The homogeneous transformation matrix ${}^0_A\mathbf{T}$, taking into account motion of the system $\{A\}$ in $\{\cdot\}$, depends on time. It is to be noticed that if $\tilde{\mathbf{r}} = [\tilde{x}, \tilde{y}, \tilde{z}, 1]^T$ is a vector describing the coordinates of dm mass (point) in the local system $\{\cdot\}$ connected to any part of the system. The coordinates of such a mass in the system $\{\cdot\}$ may be described as

$$\mathbf{r} = {}^0_A\mathbf{T}(t)\overline{\mathbf{T}}(\mathbf{q})\mathbf{r}' = \mathbf{T}\mathbf{r}' \quad (3.4)$$

where $\overline{\mathbf{T}}(\mathbf{q}) = {}^A_{\{\cdot\}}\mathbf{T}(q_1, \dots, q_n)$ is transformation matrix of coordinates from the local coordinate system $\{\cdot\}'$ into the $\{A\}$ system, dependent on the generalized coordinates (q_1, \dots, q_n) of the body $\mathbf{T} = {}^0_A\mathbf{T}(t)\overline{\mathbf{T}}(\mathbf{q})$.

3.2. Crane pedestal

The crane pedestal was digitized by means of MRFEM. The number of rigid elements on which the pedestal was divided, equals $n_1 + 1$. The first rigid element (rfe(1,0)) is added to the vessel body. The generalized coordinates describing location of the second and other rigid elements modelling the pedestal with respect to its predecessors, may be presented as vectors

$$\tilde{\mathbf{q}}^{(1,i)} = [\varphi_x^{(1,i)}, \varphi_y^{(1,i)}, \varphi_z^{(1,i)}]^T = [\tilde{q}_x^{(1,i)}, \tilde{q}_y^{(1,i)}, \tilde{q}_z^{(1,i)}]^T \quad (3.5)$$

where $\varphi_x^{(1,i)}$, $\varphi_y^{(1,i)}$, $\varphi_z^{(1,i)}$ are the rotation angles presented in Fig. 3.

The vector of generalized coordinates of the “rfe” yields

$$\begin{aligned} \mathbf{q}^{(1,1)} &= \tilde{\mathbf{q}}^{(1,1)} = [q_1^{(1,1)}, q_2^{(1,1)}, q_3^{(1,1)}]^T \\ \mathbf{q}^{(1,i)} &= [\mathbf{q}^{(1,i-1)T}, \tilde{\mathbf{q}}^{(1,i)T}]^T = [q_1^{(1,i)}, q_2^{(1,i)}, \dots, q_{3i}^{(1,i)}]^T \quad i = 2, \dots, n_1 \end{aligned} \quad (3.6)$$

In accordance to the above consideration, during derivation of the equations of motion, kinetic and potential energy of the rfe(1,0) have been omitted. On the basis of equations presented in

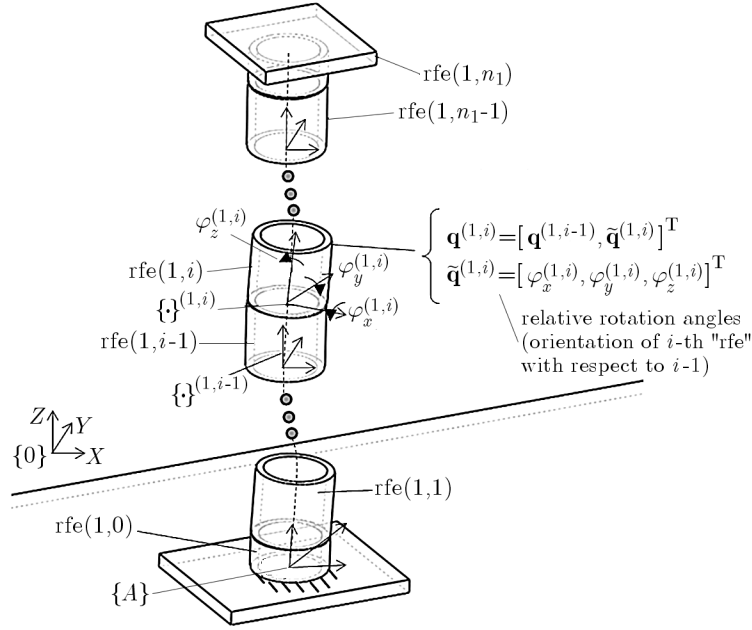


Fig. 3. Pedestal discretized by means of MRFEM

previous works, for example in Wittbrodt *et al.* (2006), the kinetic energy of the body discretized by the MRFEM can be calculated as

$$E_1 = \sum_{i=1}^{n_1} E_{(1,i)} \quad E_{(1,i)} = \frac{1}{2} \text{tr} \left\{ \dot{\mathbf{T}}^{(1,i)} \mathbf{H}^{(1,i)} \dot{\mathbf{T}}^{(1,i)\text{T}} \right\} \quad (3.7)$$

where $\mathbf{H}^{(1,i)}$ is the inertia matrix of the rigid element $(1, i)$ defined in its own coordinate system, $\mathbf{T}^{(1,i)}$ – transformation matrix from the coordinate system of rfe $\{1, i\}$ into the coordinate system $\{\cdot\}$ for $i = 1, \dots, n_1$ and

$$\mathbf{T}^{(1,i)} = \mathbf{T}^{(1,i-1)} \tilde{\mathbf{T}}^{(1,i)} = {}^0_A \mathbf{T} \tilde{\mathbf{T}}^{(1,0)} \tilde{\mathbf{T}}^{(1,1)} \dots \tilde{\mathbf{T}}^{(1,i-1)} \tilde{\mathbf{T}}^{(1,i)}$$

$\tilde{\mathbf{T}}^{(1,i)}$ – transformation matrix from the coordinate system of rfe $\{1, i\}$ into system of rfe $\{1, i-1\}$.

For the Lagrange equations, the concept of Lagrange operators is often introduced

$$\varepsilon_i(E) = \frac{d}{dt} \frac{\partial E}{\partial \dot{q}_i} - \frac{\partial E}{\partial q_i} \quad (3.8)$$

Such operators for other rfe $(1, i)$, $i = 1, \dots, n_1$, can be written in the vector form as

$$\varepsilon_{\mathbf{q}^{(1,i)}}(E_{(1,i)}) = \mathbf{A}^{(1,i)} \ddot{\mathbf{q}}^{(1,i)} + \mathbf{e}^{(1,i)} \quad (3.9)$$

where

$$\begin{aligned} \mathbf{A}^{(1,i)} &= (a_{k,j}^{(1,i)})_{k,j=1,\dots,3n_1} = \text{tr} \left\{ \mathbf{T}_k^{(1,i)} \mathbf{H}^{(1,i)} \mathbf{T}_j^{(1,i)\text{T}} \right\} \\ \mathbf{e}^{(1,i)} &= (e_k^{(1,i)})_{k=1,\dots,3n_1} = \sum_{j=1}^{3n_1} \sum_{l=1}^{3n_1} \text{tr} \left\{ \mathbf{T}_k^{(1,i)} \mathbf{H}^{(1,i)} \mathbf{T}_{j,l}^{(1,i)} \right\} \dot{q}_j^{(1,i)} \dot{q}_l^{(1,i)} \\ &\quad + \text{tr} \left\{ \mathbf{T}_k^{(1,i)} \mathbf{H}^{(1,i)} \left[{}^0_A \ddot{\mathbf{T}}^{(1,i)} + 2 {}^0_A \dot{\mathbf{T}}^{(1,i)} \right]^{\text{T}} \right\} \\ \bar{\mathbf{T}}^{(1,i)} &= \prod_{j=0}^i \tilde{\mathbf{T}}^{(1,j)} \quad \mathbf{T}_k^{(1,i)} = \frac{\partial \mathbf{T}^{(1,i)}}{\partial q_k^{(1,i)}} \quad \mathbf{T}_{j,l}^{(1,i)} = \frac{\partial}{\partial q_j^{(1,i)}} \left(\frac{\partial \mathbf{T}^{(1,i)}}{\partial q_l^{(1,i)}} \right) \end{aligned}$$

The potential energy due to gravity forces acting on rigid elements of the pedestal can be described

$$V_{(1,i)}^g = m^{(1,i)} g \boldsymbol{\theta}_3 \mathbf{T}^{(1,i)} \tilde{\mathbf{r}}_C^{(1,i)} \quad i = 1, 2, \dots, n_1 \quad (3.10)$$

where $m^{(1,i)}$ is the mass of the rfe(1, i), g – gravity acceleration, $\boldsymbol{\theta}_3 = [0, 0, 1, 0]$ $\tilde{\mathbf{r}}_C^{(1,i)}$ – vector of the element mass centre (1, i) expressed in its own coordinate system.

The corresponding derivatives, which are elements of the Lagrange equations, are

$$\frac{\partial V_{(1,i)}^g}{\partial \mathbf{q}^{(1,i)}} = \mathbf{G}^{(1,i)} \quad (3.11)$$

where

$$\mathbf{G}^{(1,i)} = (g_k^{(1,i)})_{k=1, \dots, 3n_1} \quad g_k^{(1,i)} = m^{(1,i)} g \boldsymbol{\theta}_3 \mathbf{T}_k^{(1,i)} \tilde{\mathbf{r}}_C^{(1,i)}$$

In MRFEM, the successive rfe are connected with each other by means of massless, spring-damping elements (sde). Potential energy of the elastic deformation rfe(1, i) is defined as

$$V_{(1,i)}^s = \frac{1}{2} \left(c_{i,x}^{(1)} [\varphi_x^{(1,i)}]^2 + c_{i,y}^{(1)} [\varphi_y^{(1,i)}]^2 + c_{i,z}^{(1)} [\varphi_z^{(1,i)}]^2 \right) = \frac{1}{2} \sum_{j=1}^3 c_{i,j}^{(1)} [\tilde{q}_j^{(1,i)}]^2 \quad (3.12)$$

where $c_{i,x}^{(1)}$, $c_{i,y}^{(1)}$, $c_{i,z}^{(1)}$ are the adequate coefficients of the rotational stiffness of rfe(1, i).

Equation (3.12) can be presented in the form

$$V_{(1,i)}^s = \frac{1}{2} \tilde{\mathbf{q}}^{(1,i)T} \mathbf{C}^{(1,i)} \tilde{\mathbf{q}}^{(1,i)} \quad (3.13)$$

where

$$\mathbf{C}^{(1,i)} = \text{diag} [c_{i,x}^{(1)}, c_{i,y}^{(1)}, c_{i,z}^{(1)}] = \text{diag} [c_{i,1}^{(1)}, c_{i,2}^{(1)}, c_{i,3}^{(1)}]$$

The required derivatives of the potential energy of elastic deformation have a simple form

$$\frac{\partial V_{(1,i)}^s}{\partial \tilde{\mathbf{q}}^{(1,i)}} = \mathbf{C}^{(1,i)} \tilde{\mathbf{q}}^{(1,i)} \quad (3.14)$$

It may be additionally assumed that in rfe(1, i) dissipation of energy appears

$$D_{(1,i)} = \frac{1}{2} \left(b_{i,x}^{(1)} [\dot{\varphi}_x^{(1,i)}]^2 + b_{i,y}^{(1)} [\dot{\varphi}_y^{(1,i)}]^2 + b_{i,z}^{(1)} [\dot{\varphi}_z^{(1,i)}]^2 \right) = \frac{1}{2} \sum_{j=1}^3 b_{i,j}^{(1)} [\dot{q}_j^{(1,i)}]^2 \quad (3.15)$$

where $b_{i,x}^{(1)}$, $b_{i,y}^{(1)}$, $b_{i,z}^{(1)}$ are respective damping coefficients of rfe(1, i).

Equation (3.15) may be also written as

$$D_{(1,i)} = \frac{1}{2} \dot{\tilde{\mathbf{q}}}^{(1,i)T} \mathbf{B}^{(1,i)} \dot{\tilde{\mathbf{q}}}^{(1,i)} \quad (3.16)$$

where

$$\mathbf{B}^{(1,i)} = \text{diag} [b_{i,x}^{(1)}, b_{i,y}^{(1)}, b_{i,z}^{(1)}] = \text{diag} [b_{i,1}^{(1)}, b_{i,2}^{(1)}, b_{i,3}^{(1)}]$$

and the adequate derivatives can be obtained from

$$\frac{\partial D_{(1,i)}}{\partial \dot{\tilde{\mathbf{q}}}^{(1,i)}} = \mathbf{B}^{(1,i)} \dot{\tilde{\mathbf{q}}}^{(1,i)} \quad (3.17)$$

3.3. King frame – slewing part

Let us define the following vector of the generalized coordinates for the slewing part

$$\mathbf{q}^{(2)} = [\mathbf{q}^{(1,n_k)^T}, \varphi_z^{(2)}]^T = [q_1^{(2)}, q_2^{(2)}, \dots, q_{n_2}^{(2)}]^T \quad (3.18)$$

where φ_z is the angle of rotation of the slewing part with respect to the pedestal.

The kinetic energy of the slewing part can be described as

$$E_2 = \frac{1}{2} \text{tr} \left\{ \dot{\mathbf{T}}^{(2)} \mathbf{H}^{(2)} \dot{\mathbf{T}}^{(2)T} \right\} \quad (3.19)$$

where $\mathbf{H}^{(2)}$ is the inertial matrix of the slewing part.

The Lagrange operators for the slewing part are formulated in the form

$$\varepsilon_{\mathbf{q}^{(2)}}(E_2) = \mathbf{A}^{(2)} \ddot{\mathbf{q}}^{(2)} + \mathbf{e}^{(2)} \quad (3.20)$$

where

$$\begin{aligned} \mathbf{A}^{(2)} &= (a_{i,l}^{(2)})_{i,l=1,\dots,n_2} = \text{tr} \left\{ \mathbf{T}_i^{(2)} \mathbf{H}^{(2)} \mathbf{T}_l^{(2)T} \right\} \\ \mathbf{e}^{(2)} &= (e_i^{(2)})_{i=1,\dots,n_2} = \text{tr} \left\{ \mathbf{T}_i^{(2)} \mathbf{H}^{(2)} \left[{}_A^0 \ddot{\mathbf{T}} \overline{\mathbf{T}}^{(2)} + 2 {}_A^0 \dot{\mathbf{T}} \sum_{j=1}^{n_2} \overline{\mathbf{T}}_j^{(2)} \dot{q}_j^{(2)} + \sum_{l=1}^{n_2} \sum_{j=l}^{n_2} \delta_{l,j} \mathbf{T}_{l,j}^{(2)} \dot{q}_l^{(2)} \dot{q}_j^{(2)} \right]^T \right\} \\ \delta_{l,j} &= \begin{cases} 1 & \text{for } l = j \\ 2 & \text{for } l \neq j \end{cases} \\ \overline{\mathbf{T}}^{(2)} &= \tilde{\mathbf{T}}^{(1,0)} \tilde{\mathbf{T}}^{(1,1)} \dots \tilde{\mathbf{T}}^{(1,n_1)} \mathbf{T}_2^{(1,n_1)} \end{aligned}$$

and $\mathbf{T}_2^{(1,n_1)}$ is the transformation matrix from the coordinate system of slewing part {2} to the last “rfe” coordinate system of pedestal {1, n_1 }.

The potential energy of gravity forces of the slewing body equals

$$V_2^g = m^{(2)} g \boldsymbol{\theta}_3 \mathbf{T}^{(2)} \tilde{\mathbf{r}}_C^{(2)} \quad (3.21)$$

where $m^{(2)}$ is the mass of the slewing part, $\tilde{\mathbf{r}}_C^{(2)}$ – position vector of the mass center of the slewing part, expressed in system {2}.

The necessary derivatives are defined bellow

$$\frac{\partial V_2^g}{\partial \mathbf{q}^{(2)}} = \mathbf{G}^{(2)} \quad (3.22)$$

where

$$\mathbf{G}^{(2)} = (g_k^{(2)})_{k=1,\dots,n_2} \quad g_k^{(2)} = m^{(2)} g \boldsymbol{\theta}_3 \mathbf{T}_k^{(2)} \tilde{\mathbf{r}}_C^{(2)}$$

3.4. A-frame and boom

The A-frame is modelled by means of the MRFEM in compliance with only bending flexibility in the perpendicular direction to the plane of the A-frame. Additionally as for the pedestal, rfe(3,0) is added to the slewing part, and as a result, it does not have its own generalized coordinates, Fig. 4. The following vectors of generalized coordinates for each “rfe” of the A-frame are defined:

— one-element vectors of the flexible coordinates

$$\tilde{\mathbf{q}}^{(3,1)} = [\varphi_y^{(3,1)}] \quad \dots \quad \tilde{\mathbf{q}}^{(3,n_3)} = [\varphi_y^{(3,n_3)}] \quad (3.23)$$

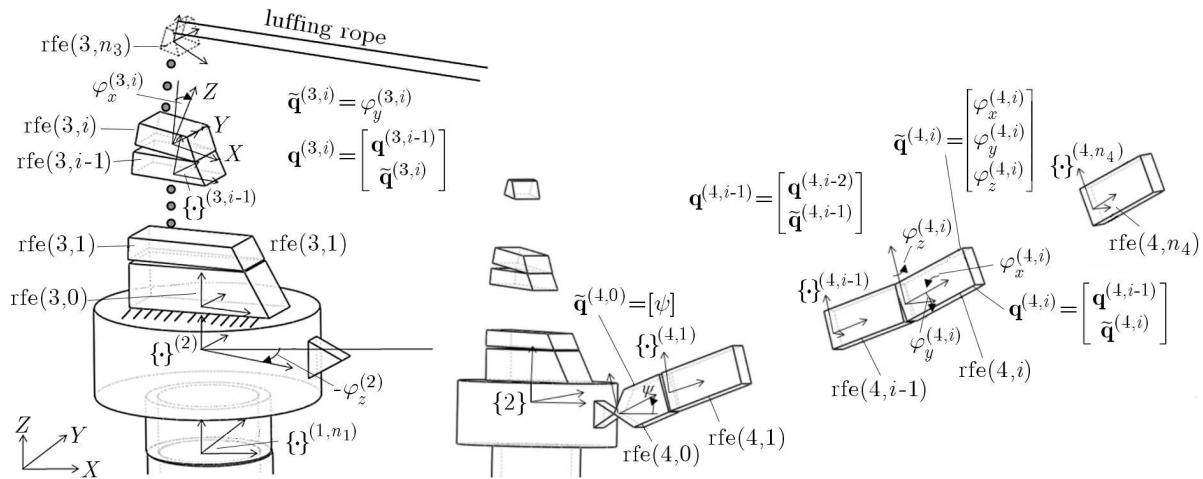


Fig. 4. Simplified model of flexible A-frame and boom

— coordinate vectors describing the position of the rigid element with respect to the base coordinate system

$$\mathbf{q}^{(3,i)} = [\mathbf{q}^{(2)\text{T}}, \tilde{\mathbf{q}}^{(3,1)\text{T}}, \dots, \tilde{\mathbf{q}}^{(3,i)\text{T}}]^\text{T} = [q_1^{(3,i)}, \dots, q_{n_2+i}^{(3,i)}]^\text{T} \quad i = 1, 2, \dots, n_3 \quad (3.24)$$

In contradistinction to the pedestal and A-frame, in the case of boom, it was assumed that there is a rotational connection between rotating part {2} and rfe(4,0), Fig. 4 – angle ψ . We can define the following vectors of generalized coordinates for the boom:

— vectors of the flexible coordinates

$$\tilde{\mathbf{q}}^{(4,0)} = [\psi] = [\varphi_y^{(4,0)}] \quad \dots \quad \tilde{\mathbf{q}}^{(4,i)} = [\varphi_x^{(4,i)}, \varphi_y^{(4,i)}, \varphi_z^{(4,i)}]^\text{T} \quad i = 1, 2, \dots, n_4 \quad (3.25)$$

— coordinate vectors describing the position of the rigid element with respect to the base coordinate system

$$\mathbf{q}^{(4,i)} = [\mathbf{q}^{(2)\text{T}}, \tilde{\mathbf{q}}^{(4,0)\text{T}}, \dots, \tilde{\mathbf{q}}^{(4,i)\text{T}}]^\text{T} = [q_1^{(4,i)}, \dots, q_{3i+n_2+1}^{(4,i)}]^\text{T} \quad i = 0, 1, \dots, n_4 \quad (3.26)$$

The necessary elements of the Lagrange equations related to the A-frame and boom subsystems were calculated in the same way as presented in Section 3.2.

3.5. The model of shock absorber

The model of the shock absorber is presented in Fig. 5. Its basic element is sheave (3) possessing the mass m_{sA} mounted to the boom by means of a parallel spring-damping system. Relative motion of sheave (3) is possible only along the longitudinal axis of the boom. The mass m_{sA} is enlarged due to movable parts of the hydraulic cylinder.

In the presented model, the characteristic shown in Fig. 6a was assumed for the elastic element. It represents the characteristic $c_{SA} = c_{SA}(x)$. The curve given in Fig. 6a can be described as follows

$$y = \begin{cases} S + c(x - \Delta) & \text{for } x \geq a\Delta \\ kx + \alpha x^2 e^{\beta x} & \text{for } 0 \leq x < a\Delta \\ -S + c(x - \Delta) & \text{for } x \leq -a\Delta \\ kx - \alpha x^2 e^{-\beta x} & \text{for } -a\Delta < x < 0 \end{cases} \quad (3.27)$$

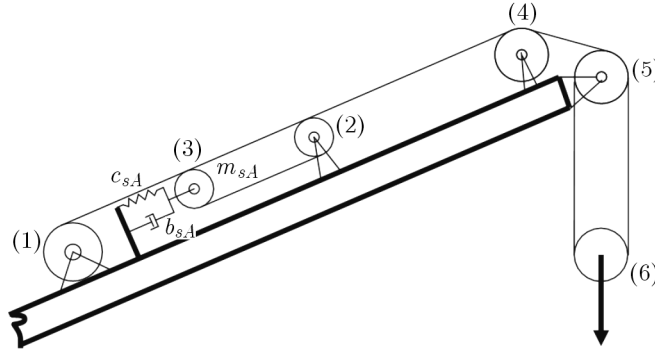


Fig. 5. Model of the shock absorber

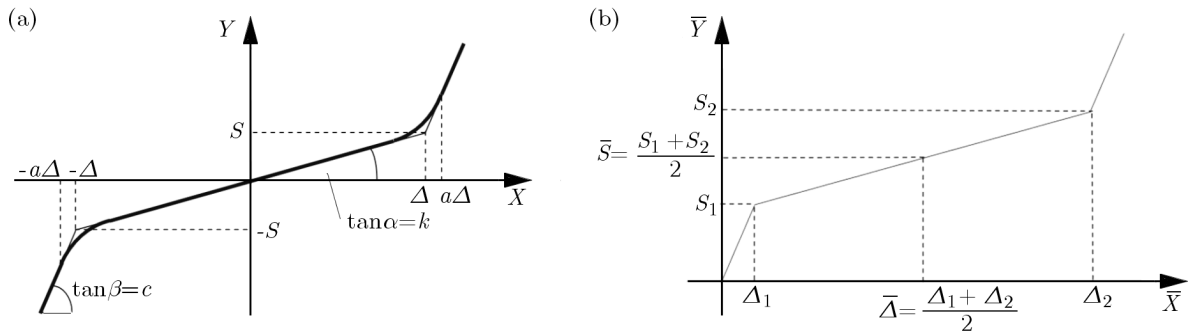


Fig. 6. Characteristic of: (a) elastic element $c_{SA} = c_{SA}(x)$, (b) shock absorber

By selecting appropriate values of α and β , one obtains smooth transition curves at the point $x = a\Delta$ (and $x = -a\Delta$). Then the following conditions must be fulfilled

$$\begin{aligned} ka\Delta + \alpha(a\Delta)^2 e^{\beta a\Delta} &= S + c(a\Delta - \Delta) = k\Delta + c(a - 1)\Delta \\ k + 2\alpha a\Delta e^{\beta a\Delta} + \alpha a^2 \Delta^2 \beta e^{\beta a\Delta} &= c \end{aligned} \tag{3.28}$$

After some transformations, parameters α and β are obtained

$$\beta = \frac{2 - a}{a\Delta(a - 1)} \quad \alpha = \sqrt{\frac{(a - 1)(c - k)}{a^2 \Delta e^{\beta a\Delta}}} \tag{3.29}$$

The shock absorber is designed in such a way that it works only under the tensioning load. Up to the value of force S_1 , the stiffness is a very high value. Within the limit of forces S_1 up to S_2 , the stiffness decreases (shock absorber working range), and beyond the force S_2 , its stiffness increases significantly. The characteristic of the elastic element from Fig. 6a must be appropriately scaled to the form shown in Fig. 6b. The shock absorber working parameters are defined by the following variables:

- S_1, S_2 – minimum/maximum force within which the shock absorber is active,
- Δ_1, Δ_2 – displacement of the shock absorber sheave corresponding to the force S_1 and S_2 ,
- a – parameter specifying where the point of curvilinear part of the characteristic is becoming rectilinear, $a > 1$,
- α, β – parameters defining the shape of the characteristic described by equation (3.29).

Form Fig. 6b, it is easy to read that the constants c and k are described by means of

$$c = \frac{S_1}{\Delta_1} \quad k = \frac{S_2 - S_1}{\Delta_2 - \Delta_1} \tag{3.30}$$

and the values of x and y are determined as

$$y = \bar{y} - \bar{S} \quad x = \bar{x} - \bar{\Delta} \quad (3.31)$$

where \bar{x} , \bar{y} , $\bar{\Delta}$ and \bar{S} are shown in Fig. 6b.

3.6. Hoisting and luffing ropes

The potential energy of elastic deformation and function of energy dissipation for the hoist and luffing rope can be described by the following equations

$$V_l = \frac{1}{2} \delta c^{(l)} \Delta_l^2 \quad D_l = \frac{1}{2} \delta b^{(l)} \dot{\Delta}_l^2 \quad (3.32)$$

where

$$\delta = \begin{cases} 0 & \text{for } \Delta_l \leq 0 \\ 1 & \text{for } \Delta_l > 0 \end{cases}$$

and Δ_l is the elongation of the hoist or luffing rope, $c^{(l)}$, $b^{(l)}$ – stiffness and damping coefficients of the ropes, respectively.

Because of the possibility of significant changes in the active length of the hoist rope during crane operation, the stiffness coefficient of the hoist rope is determined by means of the expression

$$c^{(l)} = \frac{E_6 F_6}{L_{6,0} - \alpha_{(6)} r_{(6)}} \quad (3.33)$$

where $L_{6,0}$ is the initial length of the hoist rope, E_6 , F_6 – Young's modulus and cross section of the wire rope core, respectively, $\alpha_{(6)}$ – rotation angle of the hoist winch drum, $r_{(6)}$ – radius of the hoist which drum.

The stiffness coefficient $c^{(l)}$ of the luffing rope is considered as a constant value. A method of determination of the necessary derivatives of equations (3.32) was described by Maczyński (2008), which was applied in this work as well.

3.7. Load

The load was modelled as a material point. The weight of the hook block was added to the weight of the load. The vector of generalized coordinates is defined as

$$\mathbf{q}^{(L)} = [x^{(L)}, y^{(L)}, z^{(L)}]^T = [q_1^{(L)}, q_2^{(L)}, q_3^{(L)}]^T \quad (3.34)$$

The kinetic and potential energy of the load are described by means of

$$E_L = \frac{1}{2} m^{(L)} (\dot{x}^{(L)2} + \dot{y}^{(L)2} + \dot{z}^{(L)2}) \quad V_L^g = m^{(L)} g z^{(L)} \quad (3.35)$$

where $m^{(L)}$ is the mass of the load. On this basis it is possible to write

$$\varepsilon_{\mathbf{q}^{(L)}} = \mathbf{A}^{(L)} \ddot{\mathbf{q}}^{(L)} \quad \frac{\partial V_L^g}{\partial \mathbf{q}^{(L)}} = [0, 0, m^{(L)} g]^T \quad (3.36)$$

where $\mathbf{A}^{(L)} = \text{diag} [m^{(L)}, m^{(L)}, m^{(L)}]$.

The computer program allowed simulation of the following cases:

- the load is in the air (water) – does not remain in contact with the deck of the supply vessel,
- the load remains stationary on board of the supply vessel; its coordinates are defined by motion of the supply vessel,
- the load is permanently connected to the supply vessel (e.g. frozen).

3.8. Drive systems

The slewing, hoisting and luffing drive systems are modelled as kinematic inputs. Therefore, the following function is known

$$\phi_d = \phi_d(t) \quad (3.37)$$

where ϕ_d is respectively the slewing angle, hoisting or luffing winch rotation angle.

From the perspective of planned applications of the model presented, the hoisting machinery is one of the most significant drive systems. Therefore, the second method of its modelling, using force excitation, is carried out. Based on the analysis of literature (e.g., Osiński *et al.*, 2004) as well as the gained experience from crane operators and designers, the hoist winch characteristic was assumed as shown in Fig. 7.

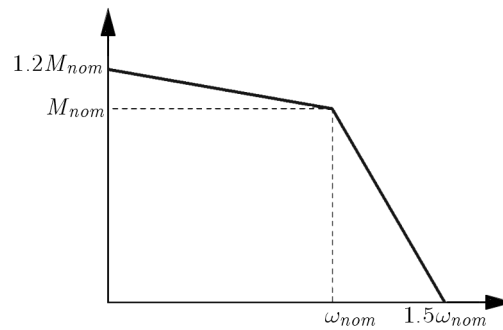


Fig. 7. Hoist winch characteristic

3.9. Agregation of the equations of motion

Substituting to Lagrange equations (3.1), the equations of motion of the crane can be written as

$$\mathbf{A}\ddot{\mathbf{q}} = \mathbf{F} \quad (3.38)$$

where \mathbf{A} is the inertia matrix, \mathbf{q} – vector of generalized coordinates, \mathbf{F} – right-hand side vector; its elements are designated as the partial derivatives of the kinetic energy, potential forces of gravity and flexibility, function of energy dissipation, etc.

Equations (3.38) were solved by a computer program using the Runge-Kutta method of the fourth order with fixed step integration. Before the integration of (3.38), initial conditions were calculated by solving the above equations assuming $\ddot{\mathbf{q}} = \dot{\mathbf{q}} = \mathbf{0}$. The resulting system of nonlinear algebraic equations was solved using Newton's method.

4. Numerical calculations

Exemplary simulation results obtained from the developed computer program are presented in this Section. Two load cases are considered: LC-1: hoisting of the load from the stationary deck, and LC-2: hoisting from the deck whose movement is described by the function

$$z_P = \frac{3}{4} \sin\left(\frac{2\pi}{6}t\right) \text{ m} \quad (4.1)$$

A load of 18000 kg (including the wire rope and hook block mass) is lifted from the supply boat deck. Assuming that the wire rope is loose at the beginning of the cycle (by a length of 1 m),

some dynamic overload can be expected. The hoisting speed is assumed 0.4 m/s for quadruple operation, with the drum rotation characteristics consistent with Fig. 7. The shock absorber was defined by the following parameters: $S_1 = 97\,500\text{ N}$, $S_2 = 1.4S_1$, $\Delta_1 = 0.02\text{ m}$, $\Delta_2 = 0.52\text{ m}$, $a = 1.1$.

Plots presented in Figs. 8 and 9 present time courses of the main hoist wire tension force, luffing wire force and z -coordinate of the load during lifting operation. Two crane models: working with and without the shock absorber are compared. The whole crane structure was assumed as rigid.

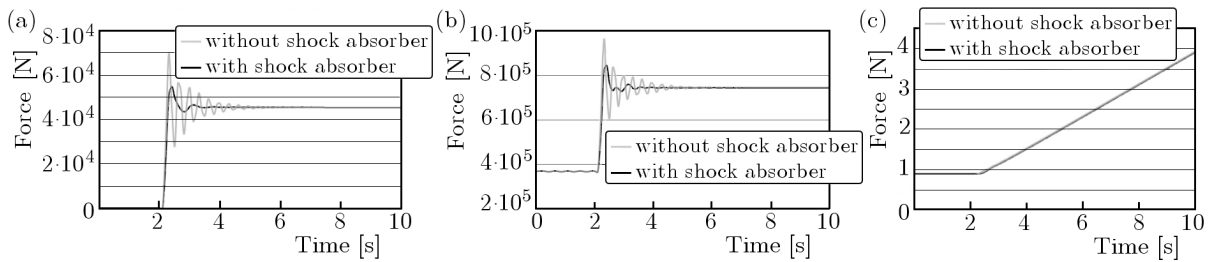


Fig. 8. LC-1 load case results: (a) hoist rope force, (b) luffing rope force, (c) z coordinate of the load

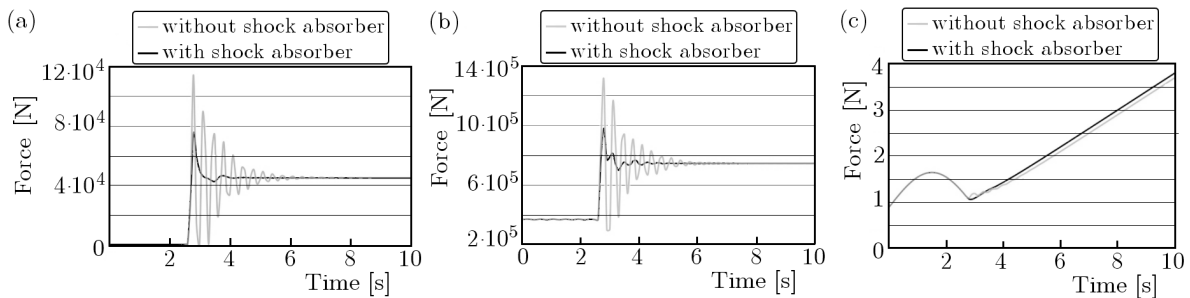


Fig. 9. LC-2 load case results: (a) hoist rope force, (b) luffing rope force, (c) z coordinate of the load

The conditions assumed in the presented examples are rather theoretical – the winch acceleration during the first phase (when the rope is loose) makes a high dynamic peak load when the wire is suddenly pretensioned. However, this scenario is simulated in order to show how effective the shock absorber could be. In some cases, without such a system, makes the life time of it much shorter.

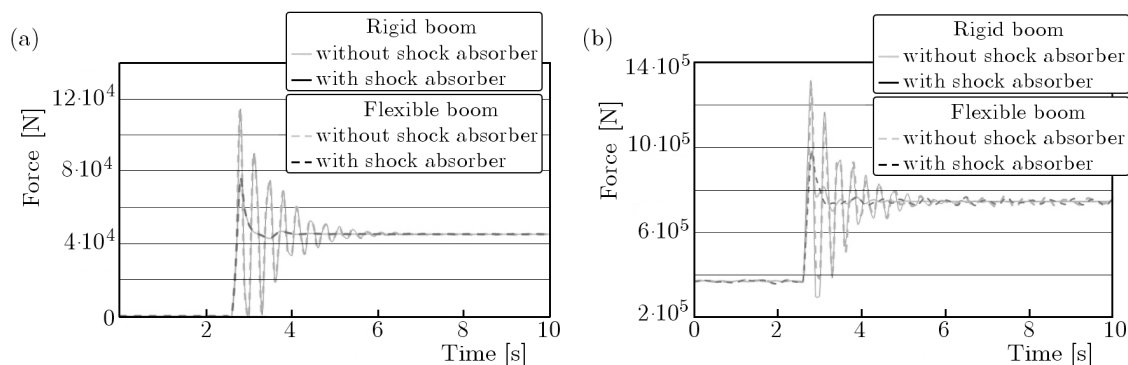


Fig. 10. LC-2 load case, comparison of the results with rigid and flexible crane boom: (a) hoist rope force, (b) luffing rope force

The plots shown in Fig. 10 were obtained for the load case LC-2, considering the flexible boom. The results for the rigid crane boom were compared with those obtained with the flexible structure. Discretization of the crane boom was performed using $n_4 = 7$ rigid finite elements.

5. Summary

The results of simulations performed using the crane model having a shock absorber installed confirm a significant decrease of the dynamic overload experienced by the structural systems. Application of the shock absorber subsystem in real constructions would allow the crane to work in much more difficult conditions. Without such systems, the same crane has to be de-rated, which would make it in a higher sea state less efficient handling tool, causing that the whole vessel or platform can not perform planned lifts until the weather conditions improve. Consequently, the load chart of a crane equipped with a system decreasing dynamic loads will be much different from the same construction without such a device. Therefore, proper working of shock absorbers is very important in the offshore cranes.

The flexibility of the boom has a small influence on the obtained results. Some slight differences are observed in the time history of the luffing rope force. It therefore appears that, for preliminary calculations or for test purposes, the flexibility of the boom can be omitted. On the basis of a model with a few degrees of freedom, an engineer obtains a quick software tool, supporting him during the design process. The calculation model presented enable us to determine the crane overload in various working conditions. That makes it possible to predict limiting weather conditions for a given crane design and specific operation scenarios. Implementation of the model in a standalone desktop application makes it attractive for various conceptual *ad-hoc* analyses.

References

1. ADAMIEC-WÓJCIK I., FAŁAT P., MACZYŃSKI A., WOJCIECH S., 2009, Load stabilisation an A-frame – a type of an offshore crane, *The Archive of Mechanical Engineering*, **56**, 1, 37-59
2. BALACHANDRAN B., LI Y.Y., FANG C.C., 1999, A mechanical filter concept for control of non-linear crane-load oscillations, *Journal of Sound and Vibrations*, **228**, 651-682
3. COZIJN J.L., VAN DER WAL R.J., DUNLOP C., 2008, Model testing and complex numerical simulations for offshore installation, *Proceeding of the 8th International Offshore and Polar Engineering Conference*, Vancouver, **I**, 137-147
4. ELLERMANN K., KREUZER E., 2003, Nonlinear dynamics in the motion of floating cranes, *Multibody System Dynamics*, **9**, 4, 377-387
5. ELLERMANN K., KREUZER E., MARKIEWICZ M., 2002, Nonlinear dynamics of floating cranes, *Nonlinear Dynamics*, **27**, 2, 107-183
6. ELLERMANN K., KREUZER E., MARKIEWICZ M., 2003, Nonlinear primary resonances of a floating crane, *Meccanica*, **38**, 5-18
7. FAŁAT P., 2004, Dynamic analysis of a sea crane of an A-frame type, PhD Thesis, Bielsko-Biała [in Polish]
8. LI Y.Y., BALACHANDRAN B., 2001, Analytical study of a system with a mechanical filter, *Journal of Sound and Vibration*, **247**, 633-653
9. MACZYŃSKI A., 2005, *Positioning and Stabilization of the Load for jib Cranes*, University of Bielsko-Biała [in Polish]
10. MACZYŃSKI A., WOJCIECH S., 2009, The influence of stabilization of load positioning in an offshore crane on taut-slack phenomenon in a rope, *The Archive of Mechanical Engineering*, **LVI**, 3, 279-290
11. MASOUD Y.N., 2000, A control system for the reduction of cargo pendulation of ship-mounted cranes, Virginia Polytechnic Institute and State University, PhD Thesis, Blacksburg, Virginia
12. MASOUD Z.N., NAYFEH A.H., MOOK D.T., 2004, Cargo pendulation reduction of ship-mounted cranes, *Nonlinear Dynamics*, **35**, 3, 299-311

13. OSIŃSKI M., MACZYŃSKI A., WOJCIECH S., 2004, The influence of ship's motion in regular wave on dynamics of an offshore crane, *The Archive of Mechanical Engineering*, **51**, 131-163
14. OSIŃSKI M., WOJCIECH S., 1994, Dynamic of hoisting appliances in marine conditions, *Machine Vibration*, **3**, 76-84
15. OSIŃSKI M., WOJCIECH S., 1998, Application of nonlinear optimisation methods to input shaping of the hoist drive of an off-shore crane, *Nonlinear Dynamics*, **17**, 369-386
16. PEDRAZZI C., BARBIERI G., 1998, LARSC: Launch and recovery smart crane for naval ROV handling, *13th European ADAMS Users' Conference*, Paris
17. SCHAUB H., 2008, Rate-based ship-mounted crane payload pendulation control system, *Control Engineering Practice*, **16**, 132-145
18. URBAŚ A., SZCZOTKA M., MACZYŃSKI A., 2010, Analysis of movement of the BOP crane under sea weaving conditions, *Journal of Theoretical and Applied Mechanics*, **48**, 677-70
19. WITTBRODT E., ADAMIEC-WÓJCIK I., WOJCIECH S., 2006, *Dynamics of Flexible Multibody Systems*, Springer
20. WITZ J.A., 1995, Parametric excitation of crane loads in moderate sea states, *Ocean Engineering*, **22**, 4, 411-420

Research is financed from the project N N502 464934

Wpływ układu anty-przeciążeniowego liny na dynamikę kolumnowego żurawia morskiego

Streszczenie

Żurawie montowane na statkach i platformach należą do grupy najczęściej wykorzystywanych urządzeń związanych z techniką morską. W procesie projektowania struktury i doboru mechanizmów napędowych tych maszyn szczególną uwagę poświęca się znaczącym ruchom unoszenia spowodowanym falowaniem morza. Ponieważ prace przeładunkowe muszą być wykonywane w warunkach intensywnego falowania, żurawie te są poddane znacznie większym siłom dynamicznym, niż odpowiadające im żurawie pracujące w warunkach lądowych. Są one wyposażane w różne systemy anty-przeciążeniowe, redukujące gwałtowne siły dynamiczne pojawiające się w trakcie podnoszenia ładunku. Jednym z takich układów jest urządzenie działające na zasadzie podobnej do amortyzatora. W pracy zaprezentowano model matematyczny umożliwiający przeprowadzanie analiz dynamicznych żurawi offshore wyposażonych w systemy anty-przeciążeniowe. Wykonano przykładowe symulacje numeryczne obrazujące efektywność działania układu w trakcie przykładowej operacji podnoszenia ładunku w warunkach powodujących znaczące przeciążenia liny nośnej.

Manuscript received January 1, 2011; accepted for print December 7, 2011